European Review for Medical and Pharmacological Sciences 2020; 24: 843-850

MiR-29 inhibits neuronal apoptosis in rats with cerebral infarction through regulating Akt signaling pathway

W. RONG[1], L. YANG[2], C.-Y. LI[1], X.-T. WU[1], Z.-D. ZHOU[1], W.-L. ZHU[1], Y. YAN[1]

[1]Department of Neurology, the Second Affiliated Hospital of Kunming Medical University, Kunming, China
[2]Kunming Medical University, Kunming, China

Abstract. – OBJECTIVE: The aim of this study was to explore the influence of micro ribonucleic acid (miR)-29 on neuronal apoptosis in rats with cerebral infarction by regulating the protein kinase B (Akt) signaling pathway.

MATERIALS AND METHODS: A total of 36 Sprague-Dawley rats were randomly divided into three groups, including: Sham group (n=12), Model group (n=12), and Inhibitor group (n=12). Common carotid artery, external carotid artery, and internal carotid artery were only exposed in the Sham group. However, the ischemia-reperfusion model was established by the suture method in the other two groups. After modeling, artificial cerebrospinal fluid was injected into the lateral ventricle in the rats of the Sham and Model groups. Similarly, miR-29 inhibitor was injected into the lateral ventricle in the rats of the Inhibitor group. At 24 h postoperatively, the sampling was performed. Zea-Longa score was used to evaluate the neurological deficit of rats. Meanwhile, the expressions of B-cell lymphoma 2 (Bcl-2) and Bcl-2 associated X protein (Bax) in cerebral tissues were detected *via* immunohistochemistry. The protein expression levels of Akt and phosphorylated Akt (p-Akt) were determined using Western blotting. Furthermore, the expression of miR-29 and cell apoptosis were detected *via* quantitative Polymerase Chain Reaction (qPCR) and terminal deoxynucleotidyl transferase (TdT) dUTP nick-end labeling (TUNEL) assay, respectively.

RESULTS: Compared with Sham group, Model, and Inhibitor groups had substantially raised the Zea-Longa scores ($p<0.05$). The Zea-Longa score in the Model group was markedly lower than that of the Inhibitor group ($p<0.05$). The positive expression level of Bax was remarkably upregulated ($p<0.05$). However, the positive expression level of Bcl-2 declined dramatically in both Model group and Inhibitor group when compared with the Sham group ($p<0.05$). Besides, the Model group exhibited significantly lower positive expression level of Bax and higher positive expression level of Bcl-2 than the Inhibitor group ($p<0.05$). The relative protein expression level of p-Akt markedly increased in the Model and Inhibitor groups when compared with the Sham group ($p<0.05$). However, it was considerably higher in the Model group than that of the Inhibitor group ($p<0.05$). In comparison with the Sham group, both Model group and Inhibitor group exerted substantially elevated expression level of miR-29 ($p<0.05$). The relative expression level of miR-29 in the Model group was significantly upregulated when compared with the Inhibitor group ($p<0.05$). The apoptosis rate of cells in both Model group and Inhibitor group was markedly higher than that of the Sham group ($p<0.05$). Furthermore, the Model group showed remarkably lower apoptosis rate than the Inhibitor group ($p<0.05$).

CONCLUSIONS: MiR-29 inhibits neuronal apoptosis in cerebral infarction rats by upregulating the Akt signaling pathway, thereby serving as a protector.

Key Words:
MiR-29, Cerebral infarction, Akt signaling pathway, Apoptosis.

Introduction

Cerebral infarction has become one of the most common cerebrovascular diseases clinically, which is due to the reason that the aging of the population is getting worse, and people's lifestyles are changing. Patients with cerebral infarction tend to have sequelae, including speech dysfunction, limb motor dysfunction, and sensory dysfunction. This may lead to a loss of labor ability, inability to live independently, and depression. It has been found that cerebral infarc-

Corresponding Author: Yong Yan, MM; e-mail: yxy968914@sina.com

tion seriously affects the life quality of patients and poses a heavy burden to their family and the society[1,2]. In severe cases, cerebral infarction can even contribute to deaths, resulting in its high disability and mortality rates. Therefore, it is of great significance to effectively prevent and treat cerebral infarction and to reduce neurological deficit-induced sequelae after cerebral infarction[3,4].

Cell apoptosis is a kind of programmed cell death. It acts as a crucial pathological reaction after cerebral infarction, showing an important influence on the repair of the nervous system. Therefore, the degree of neuronal apoptosis after cerebral infarction can affect the neurological deficit to a certain extent[5,6]. Furthermore, effectively resisting neuronal apoptosis at early stages is considered to be one of the key steps for cerebral infarction treatment.

As an important cell signal transduction pathway, the protein kinase B (Akt) signaling pathway acts as a pivotal mediator in numerous processes, including cell proliferation, differentiation, apoptosis, and necrosis. Meanwhile, it plays vital roles in the nervous system injury repair and remodeling[7,8]. Many studies[9] have demonstrated that Akt signaling pathway is a canonical anti-apoptosis pathway that can be activated by injurious stimuli to inhibit cell apoptosis after injury. Micro ribonucleic acid (miR)-29 is a non-coding RNA in organisms. It has been indicated to regulate several downstream signaling pathways, thereby exerting such effects as anti-apoptosis. However, its anti-apoptotic mechanism remains unclear. The aim of the present study was to explore the influence of miR-29 on neuronal apoptosis in cerebral infarction rats by regulating the Akt signaling pathway.

Materials and Methods

Laboratory Animals

A total of 36 specific pathogen-free laboratory Sprague-Dawley (SD) rats aged 1-month-old [Shanghai SLAC Laboratory Animal Co., Ltd., certificate No.: SCXK (Shanghai, China) 2014-0003] were enrolled in this investigation. All rats were fed with a normal diet and sterile filtered water daily in the Experimental Animal Center, with a 12-12 h light-dark cycle and normal room temperature and humidity. This study was approved by the Animal Ethics Committee of Kunming Medical University Animal Center.

Experimental Reagents and Instruments

The main reagents were: miR-29 inhibitor (GenePharma Co., Ltd., Shanghai, China), primary antibodies: anti-Akt antibody, anti-phosphorylated Akt (p-Akt) antibody, anti-B-cell lymphoma 2 (Bcl-2) antibody and anti-Bcl-2 associated X protein (Bax) antibody and secondary antibodies (Abcam, Cambridge, MA, USA), immunohistochemistry kit, AceQ quantitative polymerase chain reaction (qPCR) SYBR Green Master Mix kit and Hi Script II Q Reverse Transcriptase SuperMix for qPCR [+genomic deoxyribonucleic acid (+gDNA) wiper] kit (Vazyme Biotechnology, Nanjing, China), optical microscope (Leica DMI 4000B/DFC425C, Wetzlar, Germany), and fluorescence quantitative PCR instrument (ABI 7500, Applied Biosystems, Foster City, CA, USA).

Animal Grouping and Treatment in Each Group

36 SD rats were randomly assigned into three groups, including: Sham group (n=12), Model group (n=12), and Inhibitor group (n=12) using a random number table. All rats were adaptively fed in the Experimental Animal Center for 7 d for subsequent experiments.

Common carotid artery, external carotid artery, and internal carotid artery were only exposed in the Sham group. However, the cerebral infarction model was prepared in the Model group and Inhibitor group. After the operation, the lateral ventricle was injected with miR-29 inhibitor dissolved in artificial cerebrospinal fluid at a concentration of 20 μmol/L in Inhibitor group. Similarly, the lateral ventricle was injected with miR-29 inhibitor and dissolved in artificial cerebrospinal fluid in the Sham and Model groups. At 24 h after operation, sampling was conducted in each group.

Preparation of Cerebral Infarction Model

After successful anesthesia *via* intraperitoneal injection of 10% chloral hydrate at a dose of 3 mL/kg, the rats were fixed in the supine position. The neck was shaved, disinfected, and covered with a sterile towel. Then, a 2 cm-long longitudinal incision was made at the anterior midline of the rat neck, followed by careful separation and exposure of the common carotid artery, external carotid artery, and internal carotid artery. Subsequently, these carotid arteries were ligated using silk threads, and the internal carotid artery was clamped using vascular forceps. Next, an intraluminal thread was inserted from the

common carotid artery and pushed slowly to the middle cerebral artery branch, with vascular forceps loosed. Then, the internal carotid artery was ligated again, and the intraluminal thread was fixed. Finally, the incision was rinsed with normal saline and sutured, while timing started. After 90 min of vascular occlusion, the intraluminal thread was slowly drawn out.

Sampling

After successful anesthesia, the samples were directly obtained from 6 rats in each group. Briefly, the cerebral tissues were directly taken out and rinsed with normal saline. Then, the samples were placed in Eppendorf (EP; Hamburg, Germany) tubes and stored at -80°C for use. The remaining 6 rats in each group were fixed by perfusion for sampling as follows: the thoracic cavity of rats was first cut open to expose the heart. Then, the left atrial appendage was perfused with 400 mL of 4% paraformaldehyde. Next, the cerebral tissues were obtained and fixed with 4% paraformaldehyde for subsequent experiments.

Zea-Longa Score

At 24 h after operation, the neurological deficit of rats was evaluated using the Zea-Longa score according to the symptoms and performance of rats. Zea-Longa score was shown in Table I.

Immunohistochemistry

Pre-paraffin-embedded tissues were first made into 5 μm-thick sections. The tissues were placed in 42°C warm water for extending, mounting, and baking, followed by preparation into paraffin-embedded tissue sections. Then, the sections were routinely de-paraffinized and dehydrated by soaking in the xylene solution and gradient ethanol successively until hydration. Subsequently, the sections were immersed in citrate buffer and heated repeatedly in a microwave oven for 3 times (heating for 3 min and braising for 5 min per time) to remove the antigen completely. After rinsing, the sections were added dropwise with endogenous peroxidase blocker. After reaction for 10 min, the sections were rinsed and sealed with goat serum for 20 min. After discarding the goat serum sealing solution, the sections were incubated with anti-Bax and anti-Bcl-2 primary antibodies (1:200) in a refrigerator at 4°C overnight. On the next day, the sections rinsed were added dropwise with the corresponding secondary antibody solution. After reaction for 10 min and fully rinsing, the sections were reacted with streptomycin avidin-peroxidase solution for 10 min. Color development was performed using DAB. Finally, the cell nuclei were counterstained using hematoxylin, and the sections were sealed and observed.

Western Blotting

Cryopreserved cerebral tissues were added with lysis buffer, bathed on ice for 1 h and centrifuged at 14,000 g for 10 min. The concentration of the extracted protein was determined by the bicinchoninic acid (BCA; Pierce, Rockford, IL, USA). After separation *via* sodium dodecyl sulphate-polyacrylamide gel electrophoresis (SDS-PAGE), the protein samples were transferred onto polyvinylidene difluoride (PVDF) membranes (Millipore, Billerica, MA, USA). Then, the membranes were incubated with sealing solution for 1.5 h, followed by incubation with primary antibodies of anti-AKT and anti-p-Akt primary antibodies (1:1,000) at 4°C overnight. On the next day, the membranes were incubated with corresponding secondary antibodies (1:1,000) at room temperature for 2 h. Immuno-reactive bands were fully developed in the dark through reaction with chemiluminescent reagent for 1 min.

Quantitative Polymerase Chain Reaction (QPCR)

Cerebral tissues were first added with ribonucleic acid (RNA) extraction reagent to extract the total RNA. Subsequently, extracted total RNA was reversely transcribed into complementary DNA (cDNA). PCR was performed in a 20 μL

Table I. Zea-Longa score.

Score	Symptoms
0 point	No neurological deficit
1 point	Mild: The right front paws cannot fully stretch when the tail is raised
2 points	Moderate: The body rotates to the left during walking
3 points	Severe: The body tumbles rightwards during walking
4 points	Unable to spontaneously walk with loss of consciousness

Table II. Primer sequences.

Name	Primer sequence
MiR-29	Forward: 5' GTGGCATTACATAGTCAGCA 3' Reverse: 5' CCCATTGGCGACAGCTTGGA 3'
GAPDH	Forward: 5' ACGGCAAGTTCAACGGCACAG 3' Reverse: 5' GAAGACGCCAGTAGACTCCACGAC 3'

system under the following conditions: reaction at 53°C for 5 min, pre-denaturation at 95°C for 10 min, denaturation at 95°C for 10 s, and annealing at 62°C for 30 s, for a total of 30 cycles. The expression level of target genes was calculated by the ΔCt method. The primer sequences used in this study were shown in Table II.

Terminal Deoxynucleotidyl Transferase (TdT) dUTP Nick-End Labeling (TUNEL) Assay

The tissues embedded in paraffin in advance were made into 5 μm-thick sections. Then, the tissues were extended, mounted, and baked in warm water at 42°C, followed by preparation into paraffin-embedded tissue sections. Subsequently, the sections were routinely de-paraffinized by immersing in the xylene solution and hydrated in gradient ethanol. After reaction with proteinase K working solution at room temperature for 15 min, the sections were rinsed. Next, they were added dropwise with TUNEL reaction mixture and reacted at room temperature for 30 min. After rinsing with washing buffer and reaction stop buffer, the sections were reacted with DAB development solution for 15 s. The sections were rinsed again, and the cell nuclei were counterstained with hematoxylin. Finally, the sections were rinsed, sealed, and observed under a microscope.

Statistical Analysis

The Statistical Product and Service Solutions (SPSS) 20.0 software (IBM Corp., Armonk, NY, USA) was used for all statistical analysis. Enumeration data were expressed as mean ± standard deviation. *t*-test, corrected *t*-test, and nonparametric test were performed for data conforming to normal distribution and homogeneity of variance, those fulfilling normal distribution and heterogeneity of variance, and those not in line with normal distribution and homogeneity of variance, respectively. One-way ANOVA was performed to compare the differences among different groups, followed by the post-hoc test (Least Significant Difference). Ranked and enumeration data were subjected to the rank-sum test and Chi-square test, respectively. $p<0.05$ was considered statistically significant.

Results

Zea-Longa Score

As shown in Figure 1, the Zea-Longa score was the lowest in the Sham group, and the highest in the Inhibitor group. Compared with the Sham group, the Zea-Longa score was dramatically raised in both Model group and Inhibitor group, displaying statistically significant differences ($p<0.05$). Meanwhile, the Model group exhibited substantially lower Zea-Longa score than that of the Inhibitor group ($p<0.05$).

Immunohistochemistry Detection Results

Tan represents a positive expression. In the present study, the Sham group exhibited fewer positive expressions of Bax, but a more positive expression of Bcl-2. However, both the Model group and Inhibitor group showed a more positive expression of Bax and fewer positive expression of Bcl-2 (Figure 2). According to the statisti-

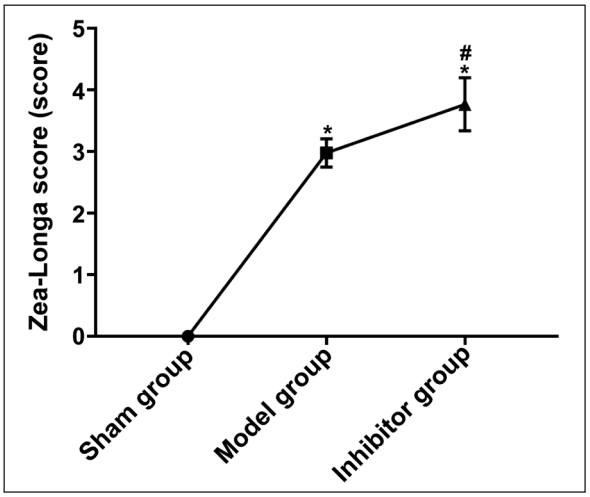

Figure 1. Zea-Longa score in each group. Note: $p^{*}<0.05$ *vs.* Sham group, and $p^{\#}<0.05$ *vs.* Model group.

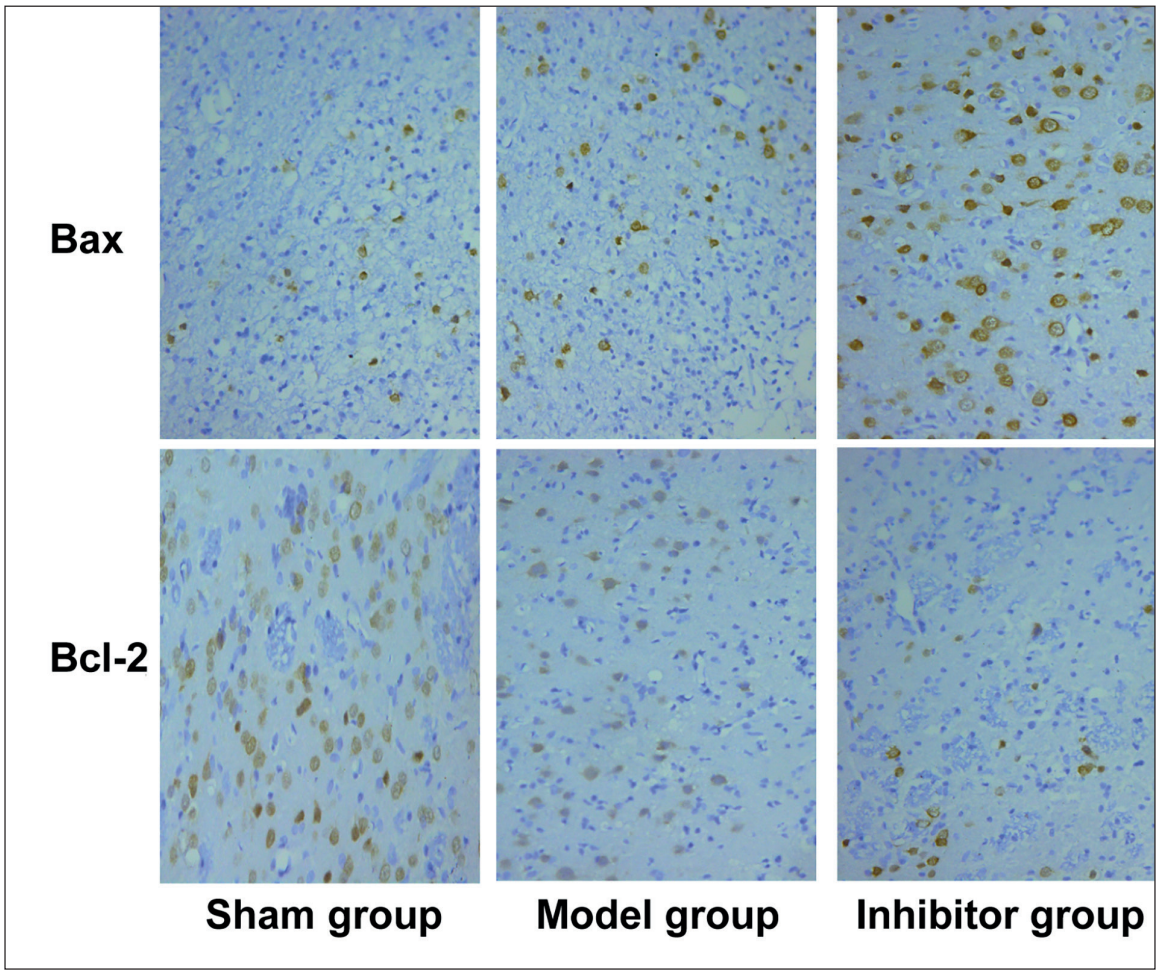

Figure 2. Expressions of Bax and Bcl-2 detected *via* immunohistochemistry (×200).

cal results (Figure 3), compared with the Sham group, the average optical density of positively expressed Bax rose substantially in the Model and Inhibitor groups ($p<0.05$). However, the average optical density of positively expressed Bcl-2 was notably downregulated in the Model and Inhibitor groups, showing statistically significant differences ($p<0.05$). Meanwhile, the Model group showed significantly lower average optical density of positively expressed Bax and higher average optical density of positively expressed Bcl-2 than the Inhibitor group, with statistically significant differences ($p<0.05$).

Relative Expression Levels of Related Proteins Determined Via Western Blotting

As shown in Figure 4, the Sham group had significantly lower protein expression level of p-Akt than the Model group and Inhibitor group

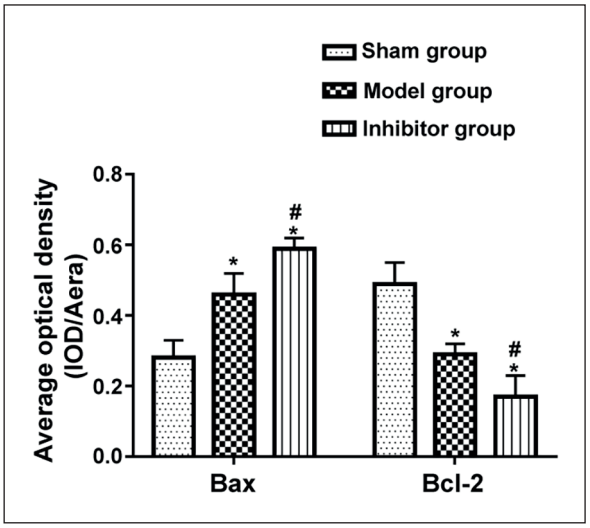

Figure 3. Average optical density of positive expressions in each group. Note: $p^{*}<0.05$ *vs.* Sham group, and $p^{\#}<0.05$ *vs.* Model group.

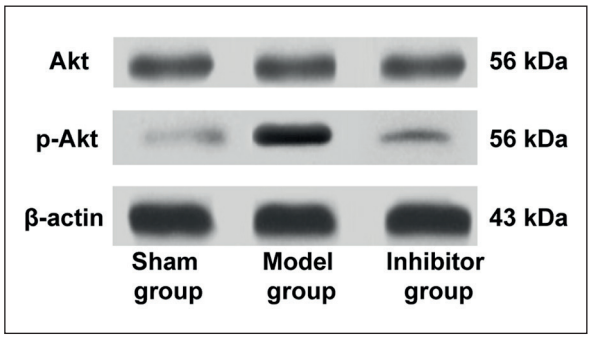

Figure 4. Expressions of related proteins detected *via* Western blotting.

(p<0.05). Statistical results indicated that the relative protein expression level of p-Akt was substantially elevated in the Model and Inhibitor groups when compared with the Sham group (p<0.05). Moreover, the relative protein expression level of p-Akt in the Model group was notably higher than that of the Inhibitor group (p<0.05). However, there were no statistically significant differences in the relative protein expression level of Akt among the three groups (p>0.05) (Figure 5).

Expression Level of mRNA Determined Via qPCR

Compared with the Sham group, the relative expression level of miR-29 was markedly upregulated in the Model and Inhibitor groups (p<0.05). Furthermore, its relative expression level in the Model group was remarkably higher than that of the Inhibitor group, showing statistically significant differences (p<0.05) (Figure 6).

Cell Apoptosis Detected Via TUNEL Assay

TUNEL assay demonstrated that both the Model group and Inhibitor group had substantially higher cell apoptosis rate than the Sham group (p<0.05). Compared with that in the Inhibitor group, the cell apoptosis rate was markedly lowered in the Model group, with a statistically significant difference (p<0.05) (Figure 7).

Discussion

Cerebral infarction often occurs in the elderly, with numerous sequelae and even death in severe cases. The morbidity, disability, mortality and recurrence rates of cerebral infarction remain high. Cell apoptosis, especially neuronal apoptosis, plays an important role in a series of complex pathological reactions after cerebral infarction. Meanwhile, it greatly affects the repair of the nervous system after cerebral infarction. This may further influence the neurological recovery in patients with cerebral infarction. Once cerebral infarction occurs, ischemia and hypoxia-induced by insufficient blood supply will activate apoptosis-associated pathways in cerebral tissues. Finally, this causes aberrant expressions of Bax and Bcl-2 that are closely related to cell apopto-

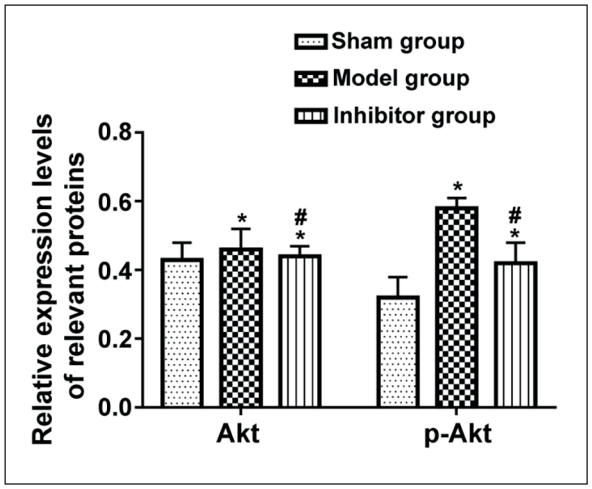

Figure 5. Relative expression levels of relevant proteins in each group. Note: p*<0.05 *vs.* Sham group, and $p^{\#}$<0.05 *vs.* Model group.

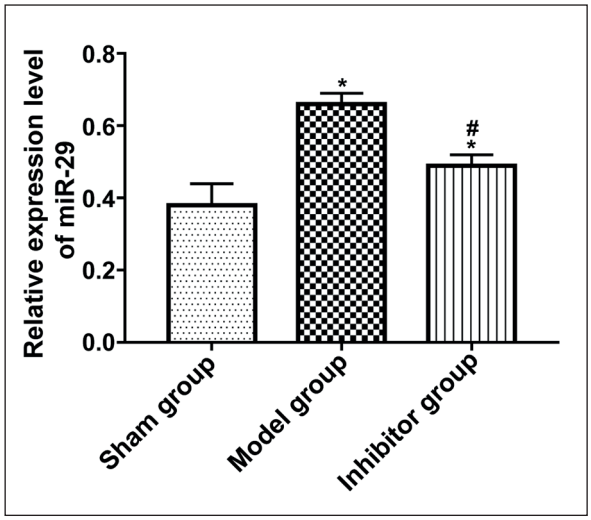

Figure 6. Relative expression level of miR-29. Note: p*<0.05 *vs.* Sham group, and $p^{\#}$<0.05 *vs.* Model group.

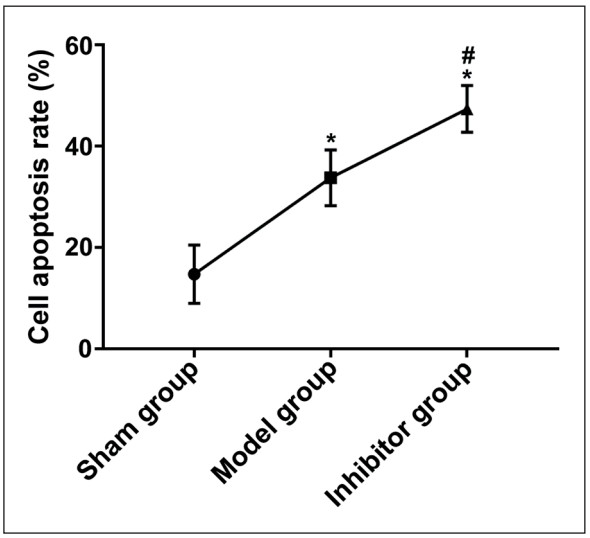

Figure 7. Cell apoptosis rate in all groups. Note: $p^{*}<0.05$ *vs.* Sham group, and $p^{\#}<0.05$ *vs.* Model group.

sis. The pro-apoptotic Bax is abnormally highly expressed, while the anti-apoptotic Bcl-2 is lowly expressed[10,11]. Meanwhile, due to the aberrant expressions of Bax and Bcl-2 in cerebral tissues, the ratio of Bax to Bcl-2 alters. The pro-apoptotic effect of Bax is more potent than the anti-apoptotic effect of Bcl-2. Ultimately, their combined action on the downstream apoptotic effector molecules aggravates neuronal apoptosis[12,13]. Neuronal apoptosis can give rise to the necrosis of large numbers of neurons after cerebral infarction. This can further adversely affect the repair of the nervous system, exacerbate cerebral infarction, and hinder the recovery of neurological function after cerebral infarction. Hence, effectively alleviating neuronal apoptosis after cerebral infarction can protect neurons well, thereby benefiting the repair of the nervous system[14].

Current studies[15,16] have found that the crucial Akt signaling pathway in the cells regulates physiological and pathological processes, such as cell proliferation, differentiation, apoptosis, and necrosis. Based on previous findings, phosphatidylinositol 3-hydroxy kinase (PI3K), the upstream molecule of Akt, can be activated by such injurious stimuli as cytokines and inflammatory factors. Active PI3K acts on phosphatidylinositol on the surface of cell membranes and activate them, thereby generating massive inositol triphosphates. Massive production of inositol triphosphates serves as the second messenger to further activate and phosphorylate Akt to form p-Akt and transduce signals. Ultimately, the Akt signaling pathway can be activated. As the key substances in the downstream of the Akt signaling pathway, both Bax and Bcl-2 play a vital role in the apoptosis pathways. These two molecules can be regulated by Akt to affect cell apoptosis[17]. In the present study, our results confirmed that the expressions of the two key apoptosis pathway molecules Bax and Bcl-2 were abnormally altered after cerebral infarction and were manifested by high expression of Bax and low expression of Bcl-2. These results suggested that dramatic apoptosis responses occurred in neurons after cerebral infarction. Moreover, the protein expression of p-Akt was significantly upregulated. This illustrated that the Akt signaling pathway was activated and involved in regulating the level of neuronal apoptosis to attenuate the influences of cerebral infarction on neurons and the nervous system. Our present study also indicated that miR-29 was aberrantly expressed in cerebral infarction, suggesting that miR-29 was implicated in several pathological reactions. After application of miR-29 inhibitor, the expression of p-Akt declined with more apoptotic neurons. This implied that miR-29 participated in the activation of the Akt signaling pathway and neuronal apoptosis after cerebral infarction. Considering the vital regulatory role of the Akt signaling pathway in neuronal apoptosis after cerebral infarction, it could be concluded that miR-29 inhibited neuronal apoptosis in rats with cerebral infarction by upregulating the Akt signaling pathway, thereby exerting a protective effect.

Conclusions

To sum up, miR-29 inhibits neuronal apoptosis in cerebral infarction rats by upregulating the Akt signaling pathway, thereby serving as a protector.

Conflict of Interest

The Authors declare that they have no conflict of interests.

References

1) Liu D, Tang ZY, Hu ZJ, Li WW, Yuan WN. MiR-940 regulates angiogenesis after cerebral infarction through VEGF. Eur Rev Med Pharmacol Sci 2018; 22: 7899-7907.
2) Peng X, Wan Y, Liu W, Dan B, Lin L, Tang Z. Protective roles of intra-arterial mild hypothermia and

arterial thrombolysis in acute cerebral infarction. Springerplus 2016; 5: 1988.

3) Zhang C, Zhao S, Zang Y, Gu F, Mao S, Feng S, Hu L, Zhang C. The efficacy and safety of Dl-3n-butylphthalide on progressive cerebral infarction: a randomized controlled STROBE study. Medicine (Baltimore) 2017; 96: e7257.

4) Yamamoto N, Satomi J, Yamamoto Y, Shono K, Kanematsu Y, Izumi Y, Nagahiro S, Kaji R. Risk factors of neurological deterioration in patients with cerebral infarction due to large-artery atherosclerosis. J Stroke Cerebrovasc Dis 2017; 26: 1801-1806.

5) Zhang J, Wang H, Yang S, Wang X. Comparison of lipid profiles and inflammation in pre- and post-menopausal women with cerebral infarction and the role of atorvastatin in such populations. Lipids Health Dis 2018; 17: 20.

6) Isahaya K, Yamada K, Yamatoku M, Sakurai K, Takaishi S, Kato B, Hirayama T, Hasegawa Y. Effects of edaravone, a free radical scavenger, on serum levels of inflammatory biomarkers in acute brain infarction. J Stroke Cerebrovasc Dis 2012; 21: 102-107.

7) Chappell WH, Steelman LS, Long JM, Kempf RC, Abrams SL, Franklin RA, Basecke J, Stivala F, Donia M, Fagone P, Malaponte G, Mazzarino MC, Nicoletti F, Libra M, Maksimovic-Ivanic D, Mijatovic S, Montalto G, Cervello M, Laidler P, Milella M, Tafuri A, Bonati A, Evangelisti C, Cocco L, Martelli AM, McCubrey JA. Ras/Raf/MEK/ERK and PI3K/PTEN/Akt/mTOR inhibitors: rationale and importance to inhibiting these pathways in human health. Oncotarget 2011; 2: 135-164.

8) Asati V, Mahapatra DK, Bharti SK. PI3K/Akt/mTOR and Ras/Raf/MEK/ERK signaling pathways inhibitors as anticancer agents: structural and pharmacological perspectives. Eur J Med Chem 2016; 109: 314-341.

9) Chin VI, Taupin P, Sanga S, Scheel J, Gage FH, Bhatia SN. Microfabricated platform for studying stem cell fates. Biotechnol Bioeng 2004; 88: 399-415.

10) Xu XH, Zhang SM, Yan WM, Li XR, Zhang HY, Zheng XX. Development of cerebral infarction, apoptotic cell death and expression of X-chromosome-linked inhibitor of apoptosis protein following focal cerebral ischemia in rats. Life Sci 2006; 78: 704-712.

11) Sun Y, Xu Y, Geng L. Caspase-3 inhibitor prevents the apoptosis of brain tissue in rats with acute cerebral infarction. Exp Ther Med 2015; 10: 133-138.

12) Wang S, Zhou J, Kang W, Dong Z, Wang H. Tocilizumab inhibits neuronal cell apoptosis and activates STAT3 in cerebral infarction rat model. Bosn J Basic Med Sci 2016; 16: 145-150.

13) Li M, Peng J, Wang MD, Song YL, Mei YW, Fang Y. Passive movement improves the learning and memory function of rats with cerebral infarction by inhibiting neuron cell apoptosis. Mol Neurobiol 2014; 49: 216-221.

14) Ji JF, Ma XH. Effect of baculovirus P35 protein on apoptosis in brain tissue of rats with acute cerebral infarction. Genet Mol Res 2015; 14: 9353-9360.

15) Sami A, Karsy M. Targeting the PI3K/AKT/mTOR signaling pathway in glioblastoma: novel therapeutic agents and advances in understanding. Tumour Biol 2013; 34: 1991-2002.

16) Li X, Wu C, Chen N, Gu H, Yen A, Cao L, Wang E, Wang L. PI3K/Akt/mTOR signaling pathway and targeted therapy for glioblastoma. Oncotarget 2016; 7: 33440-33450.

17) Yang X, Song X, Wang X, Liu X, Peng Z. Down-regulation of TM7SF4 inhibits cell proliferation and metastasis of A549 cells through regulating the PI3K/AKT/mTOR signaling pathway. Mol Med Rep 2017; 16: 6122-6127.